Available online at www.sciencedirect.com
SCIENCE DIRECT®
ELSEVIER
European Journal of Mechanics B/Fluids 22 (2003) 369–377
EUROPEAN JOURNAL OF MECHANICS B/FLUIDS

Influence of the nutation angle in gravitational settling of particles near vortices and in turbulence

Urbano Jesús Sánchez Domínguez

Dpto. C. Agroforestales, Area de Mecánica de Fluidos, Universidad de Huelva, Escuela Politécnica Superior, Campus Universitario de La Rábida, carretera Huelva-Palos de La Frontera s/n, 21819-Palos de La Frontera, Huelva, Spain

Received 10 August 2001; accepted 14 May 2003

Abstract

The knowledge of the conditions in which particles denser than fluid settle is important in many areas of engineering, environmental sciences, meteorology, etc.

For particle flows influenced by vortices, research mainly related to steady horizontal vortices has been undertaken. In this paper we determine the influence of the inclination of the vortex axis in the gravitational settling of particles.

The results obtained, in relation to the trajectories, are qualitatively similar to previous ones for horizontal vortices. The main difference is this: in a horizontal vortex particles always remain in a plane perpendicular to the vortex axis and in an inclined vortex (angle θ) particles do not remain on that plane because there is a component $v_t \cos\theta$ that takes them out.

The average fall velocity $\langle v_z \rangle$ has an asymptote to the dimensionless terminal velocity v_t; this tendency is faster as the Stokes Number St increases and as v_t decreases. A fundamental result is the following: as θ decreases, v_t is reached faster because the component of the velocity u of the Rankine vortex over the Oz direction is small and because the v_t component that tries to keep the particles in a plane perpendicular to the vortex axis is small, so the vortex takes action over the particles for a small period of time.

1. Introduction

As is known, the conditions under which particles denser than the fluid settle under gravity is important in many fields, such as meteorology, engineering or oceanography. For example, they govern the residence times of dust particles from wind erosion or manmade pollutants (Nielsen [1], Tooby et al. [2]) and the settling in estuaries of rivers (Dutoit and Sleath [3], Perkins and Sleath [4]). A knowledge of the average settling rate of small, heavy particles is also important for those cases, as well as small water droplets in clouds, ash from volcanic eruptions, or combustion. Also there are many environmental and industrial processes involving the transport of dense particles in which the formation of large-scale coherent structures in the flows is of primary importance.

Some investigations of particle behaviour near steady horizontal vortices of strength Γ, typical radius R and maximum velocity $U = \Gamma/R$ have been made. Auton [5] showed that bubbles released beneath an irrotational vortex may become trapped at the centre of the vortex and this mechanism has been used by Sene et al. [6] to investigate the transport of bubbles in free-shear layers. Perkins and Hunt [7] prove than in the case of a horizontal vortex in a gravitational field, if the particles are released from outside the vortex their falling motion is feebly inhibited but if they are introduced into the flow within the vortex their residence time is greatly enhanced. Dávila and Hunt [8] established the dimensionless parameters which govern the trajectories of the particles and they calculate the average settling velocity of particles near a horizontal Rankine vortex under gravity. They enlarged upon some works of Crowe et al. [9] and some works of Clifford et al. [10].

E-mail address: urbano.sanchez@dcaf.uhu.es (U.J. Sánchez Domínguez).

0997-7546/$ – see front matter
doi:10.1016/S0997-7546(03)00050-5

In this paper we determine the gravitational settling behaviour of particles in the case when the vortex axis is inclined at an angle with respect the horizontal plane. In this way, after establishing the equations for particle motion, computational solutions have been obtained and we have represented the particle trajectories and the average settling velocity for various values of the parameters. In the following sections we describe the results obtained.

2. Equations for particle motion

The motion of small spherical particles in a fluid is governed by a balance between the particle inertia, gravity, and drag and buoyancy forces from the relative motion of particle and fluid.

Assuming that the particle density is generally greater than the fluid density, buoyancy forces and acceleration forces are not important. Also, particle interactions are negligible at low concentrations. Therefore, if particles are sufficiently small (Maxey and Riley [11]), the only force over the fluid is the Stokes drag force, so the position $\boldsymbol{x}^*(t)$ and velocity $\boldsymbol{v}^*(t)$ at any instant are determined by Newton's second law:

$$m_p \frac{\mathrm{d}\boldsymbol{v}^*(t)}{\mathrm{d}t^*} = 6\pi a\mu\big[\boldsymbol{u}^*(\boldsymbol{x}^*, t^*) - \boldsymbol{v}^*(t^*)\big] + m_p\boldsymbol{g} \tag{2.1}$$

with m_p particle mass, a particle radius, μ fluid viscosity, g gravitational acceleration and $\boldsymbol{u}^*(\boldsymbol{x}^*, t^*)$ local fluid velocity; quantities in boldface are vectors.

The determination of the particle motion from these equations is a complex problem and we have to obtain computational solutions. We have to write Eqs. (2.1) in dimensionless form introducing suitable dimensionless parameters.

Since the direct effect of the particle inertia is to limit the response of the particle velocity to rapid changes in the local fluid velocity, this may be characterized by identifying a relative motion relaxation time scale τ_p which for a Stokes sphere (Clift et al. [12]) is

$$\tau_p = m_p/6\pi a\mu. \tag{2.2}$$

If L_0 and U_0 are the typical length and velocity of fluctuation of the flow field, then the effect of the particle inertia is determined by the dimensionless relaxation time

$$St = \tau_p U_0/L_0; \tag{2.3}$$

this is the Stokes number (Clift et al. [12]). In many contexts this ratio is small and on this basis particle inertia is often neglected (Katz [13]).

We introduce two dimensionless ratios, the Stokes number:

$$St = m_p U_0/6\pi a\mu L_0 = \tau_p U_0/L_0 \tag{2.4}$$

and the ratio of the free fall terminal velocity in still fluid to the maximum velocity in the vortex flow:

$$V_t = m_p g/6\pi a\mu U_0 = v_{tg}/U_0. \tag{2.5}$$

The Stokes number determines the importance of particle inertia such that when St is very small, inertial effects are supposedly small.

For a Rankine vortex we take L_0 as the typical radius R and U_0 as the maximum velocity so $U_0 = \Gamma/L_0$.

Using

$$\boldsymbol{v} = \frac{\boldsymbol{v}^*}{U_0}, \qquad \boldsymbol{x} = \frac{\boldsymbol{x}^*}{L_0}, \qquad t = \frac{t^* U_0}{L_0} \tag{2.6}$$

the scaled nondimensional equations of motion are

$$\begin{aligned} &\frac{\mathrm{d}\boldsymbol{x}(t)}{\mathrm{d}t} = \boldsymbol{v}(t), \\ &\frac{\mathrm{d}\boldsymbol{v}(t)}{\mathrm{d}t} = \frac{1}{St}\boldsymbol{u}(\boldsymbol{x}, t) - \boldsymbol{v}(t) + \boldsymbol{v}_t \end{aligned} \tag{2.7}$$

with initial condition

$$\begin{aligned} &\boldsymbol{x}(t=0) = \boldsymbol{x}_0, \\ &\boldsymbol{v}(t=0) = \boldsymbol{u}(\boldsymbol{x}_0, t=0) + \boldsymbol{v}_t. \end{aligned} \tag{2.8}$$

(We are assuming that the particle density is greater than fluid density and the Reynolds number of the particle is very small.)

The imposed initial condition was the simplest possible: the particles are in equilibrium with the surrounding flow conditions.

As we have already mentioned, in the case of vortices the parameters we have employed to write the equations of motion in dimensionless form are Γ, U_0 and $L_0 = \Gamma/U_0$.

Therefore the Stokes number becomes

$$St = \frac{|\beta - 1|}{k_T} \frac{d_p^2}{18\upsilon} \frac{U_0^2}{\Gamma}, \tag{2.9}$$

where β is the ratio between the particle density and the fluid density, d_p is the particle diameter and υ is the kinematic viscosity of the fluid. Since we assume in this paper that the Reynolds number of the particles based on their relative motion $v_{\text{rel}} = |v - u|$, $Re_p = v_{\text{rel}} d_p/\upsilon$ is small, to consider finite values of the particle Reynolds number we introduce k_T, the ratio between the actual drag force and the Stokes drag, defined for $Re_p = 0$ (Dávila and Hunt [8]).

We obtain computational solutions using a fourth order variable step size Runge–Kutta method [14], with a fluid velocity field described in the next section.

3. Inclined Rankine vortex velocity field

We consider the Rankine vortex. The normalised velocity field in cartesian co-ordinates related to the vortex are:

$$\vec{u} = \frac{-\Omega y_2}{1 + x_2^2/R^2 + y_2^2/R^2}\vec{i}_2 + \frac{\Omega x_2}{1 + x_2^2/R^2 + y_2^2/R^2}\vec{j}_2, \tag{3.1}$$

where R is the radius at which the maximum velocity occurs and Ω is twice the angular velocity at that radius.

To consider the inclination of the vortex, we must remember the co-ordinate transformation defined by the Euler angles: precession, nutation and own rotation (see Fig. 1). Beginning with the fixed axis $Oxyz$ and rotating them an angle Ψ, called precession angle, around the Oz axis we obtain the system $Ox1y1z1$ and rotating this system an angle θ called nutation angle, around the $Ox1$ axis we obtain the system $Ox2y2z2$. Finally we have to rotate the system around the $Oz2$ axis an angle ϕ, called own rotation angle, but we do not include it in this paper because it is not especially important to this study.

The vortex axis will be the $Oz2$ axis and we can consider any section of the vortex, for example the section situated on the $Ox2y2$ plane.

There are two options to make the study. The first one is to relate the dimensionless terminal velocity v_t to the system $Ox2y2z2$ and work with it:

$$\boldsymbol{v}_t = -v_t \boldsymbol{k} = -v_t \boldsymbol{k}_1 = -v_t(\sin\theta \boldsymbol{j}_2 + \cos\theta \boldsymbol{k}_2). \tag{3.2}$$

The second way is to relate the velocity field (3.1) to the fixed system $Oxyz$ and work with it:

$$\begin{aligned}\boldsymbol{u} = (\Omega/DEN)\big[&\boldsymbol{i}(-y\cos\theta - z\sin\theta\cos\Psi) + \boldsymbol{j}(x\cos\theta - z\sin\theta\sin\Psi)\\ &+ \boldsymbol{k}(x\sin\theta\cos\Psi + y\sin\theta\sin\Psi)\big]\end{aligned} \tag{3.3}$$

with

$$DEN = 1 + \frac{(x\cos\Psi + y\sin\Psi)^2}{R^2} + \frac{(-x\cos\theta\sin\Psi + y\cos\theta\cos\Psi + z\sin\theta)^2}{R^2}. \tag{3.4}$$

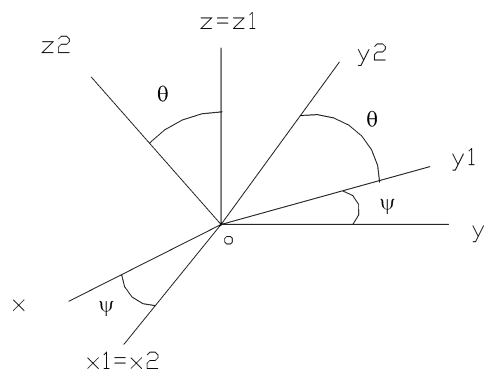

Fig. 1. Co-ordinates transformation defined by the Euler angles.

In this paper we use both options.

As the precession angle Ψ does not affect the results, in this paper we consider $\Psi = 0$ and we study the influence of the nutation angle θ.

The equilibrium points of the system (2.7), where $\mathrm{d}\boldsymbol{x}/\mathrm{d}t = \mathrm{d}^2\boldsymbol{x}/\mathrm{d}t^2 = 0$ are obtained from $u(x_E) + v_t = 0$. Working with the system $Ox2y2z2$:

$$x_{E_{1,2}} = \frac{\Omega \mp \sqrt{\Omega^2 - 4v_t^2 \sin^2\theta/R^2}}{2v_t \sin\theta/R^2}$$

as $V_t \to 0$, $\boldsymbol{x}_{E1} \to (0,0)$ while $\boldsymbol{x}_{E2} \to (R^2\Omega/v_t \sin\theta, 0)$. Dávila and Hunt [8] prove that in a horizontal vortex, x_{E1} is an unstable focus (node if $St = 0$) and x_{E2} is a saddle point of the dynamical system defined by (2.7). The only difference between a horizontal and an inclined vortex in relation to equilibrium points is that they are displaced in position due to the factor "$\sin\theta$" appearing in the formula.

4. Results

4.1. Trajectories of particles

In Fig. 2 we have plotted the trajectories of non-inertial particles ($St = 0$) for the horizontal vortex case. In this case the systems $Oxyz$ and $Ox2y2z2$ coincide.

We can observe that the trajectories are symmetric about $z = 0$ and some particles follow close trajectories around the centre of the vortex as demonstrated by Dávila and Hunt [8]. The fundamental difference with the case $\theta \neq \pi/2$ is, as we will see later, for $\theta = \pi/2$ particles always move on planes $y =$ constant because there is not any force to bring them out of that plane. Therefore the movement is 2D.

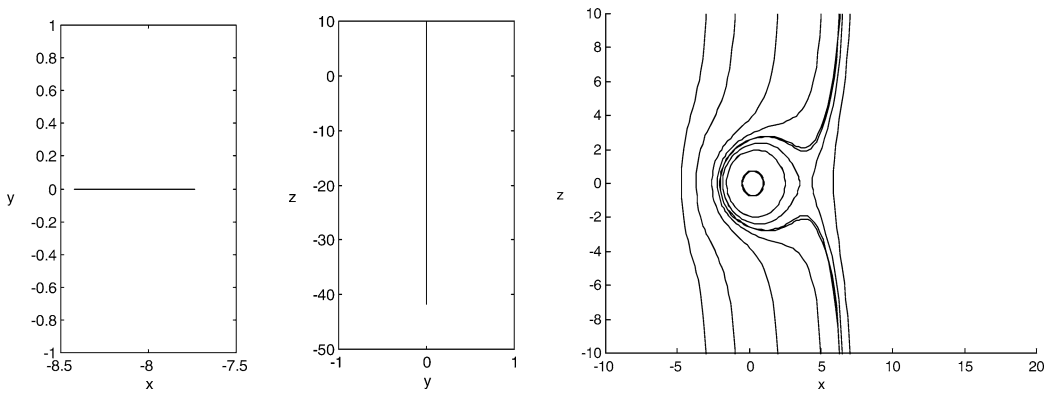

Fig. 2. Trajectories of non-inertial particles ($St = 0$) for a horizontal vortex ($\theta = \pi/2$).

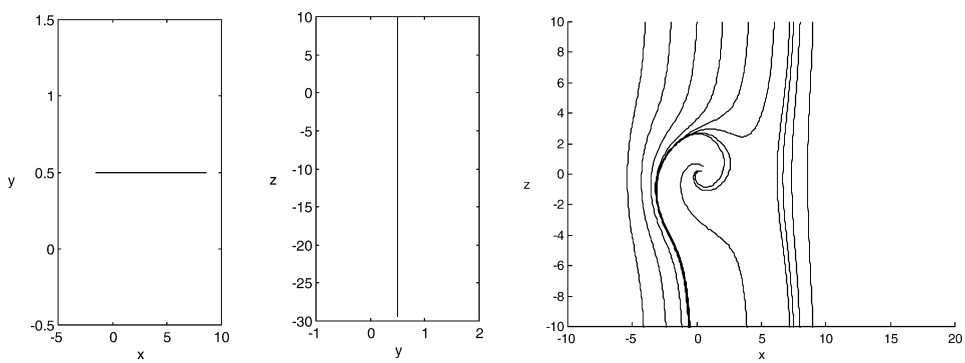

Fig. 3. Trajectories of inertial particles ($St = 0.5$) for a horizontal vortex ($\theta = \pi/2$).

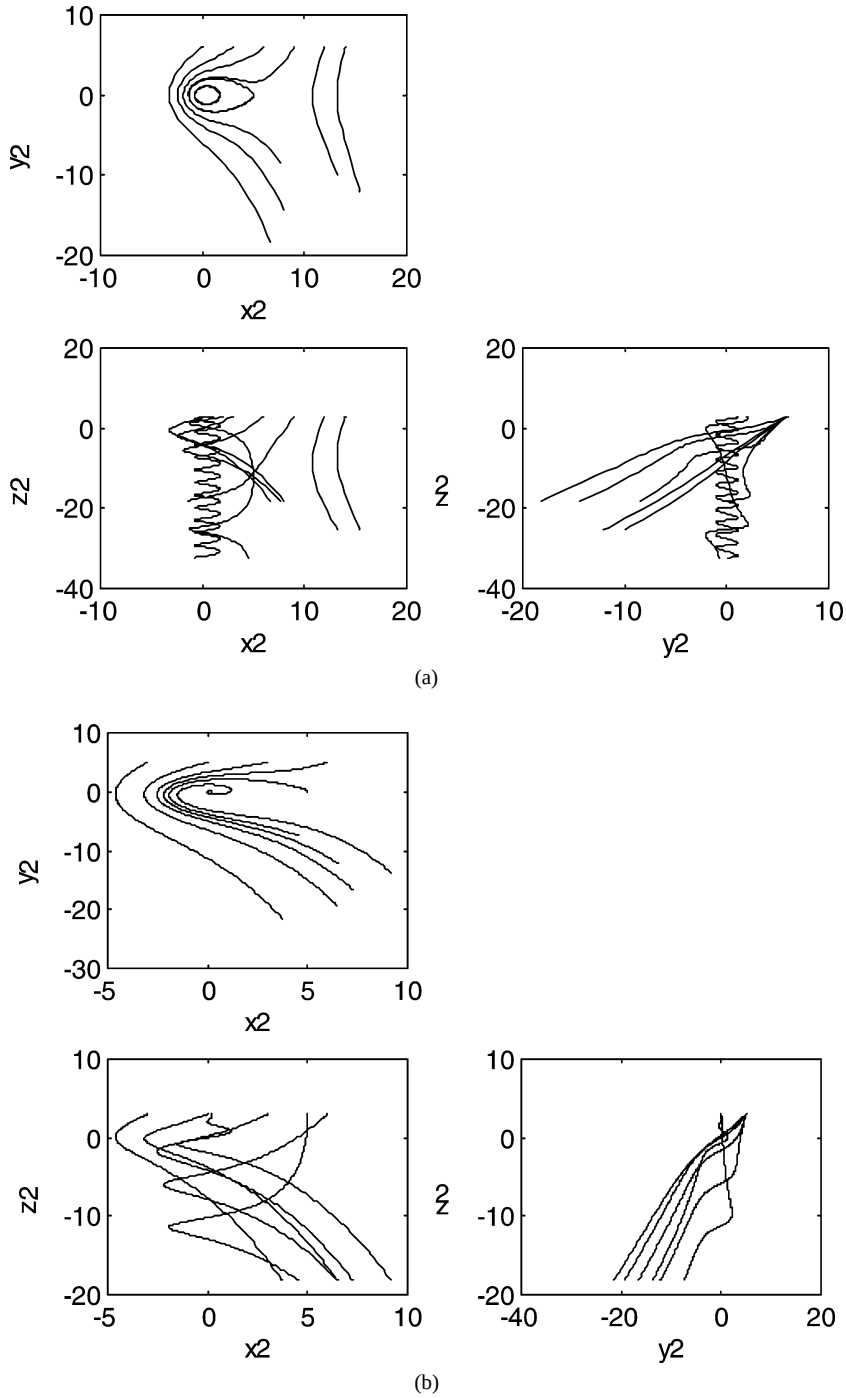

Fig. 4. Trajectories of particles. (a) $\theta = \pi/4$, $St = 0$, $v_t = 0.5$. (b) $\theta = \pi/4$, $St = 0.5$, $v_t = 0.5$.

Fig. 3 shows the trajectories of inertial particles, $St = 0.5$, for a horizontal vortex ($\theta = \pi/2$). The movement is 2D too, particles move in the plane $y =$ constant but there are no closed trajectories around $\boldsymbol{x}_{E1}$. Particles starting at this point move outwards on trajectories that are spirals because of the centrifugal inertial force so particles released inside the vortex gradually drift outward on a time scale $t = f(v_t)/Fr$ where $Fr = V_t^2 St$ is the particle Froude number and $f(v_t)$ is a function of the dimensionless terminal velocity (Perkins and Hunt [7]). According Dávila and Hunt [8] there are two limit trajectories separating

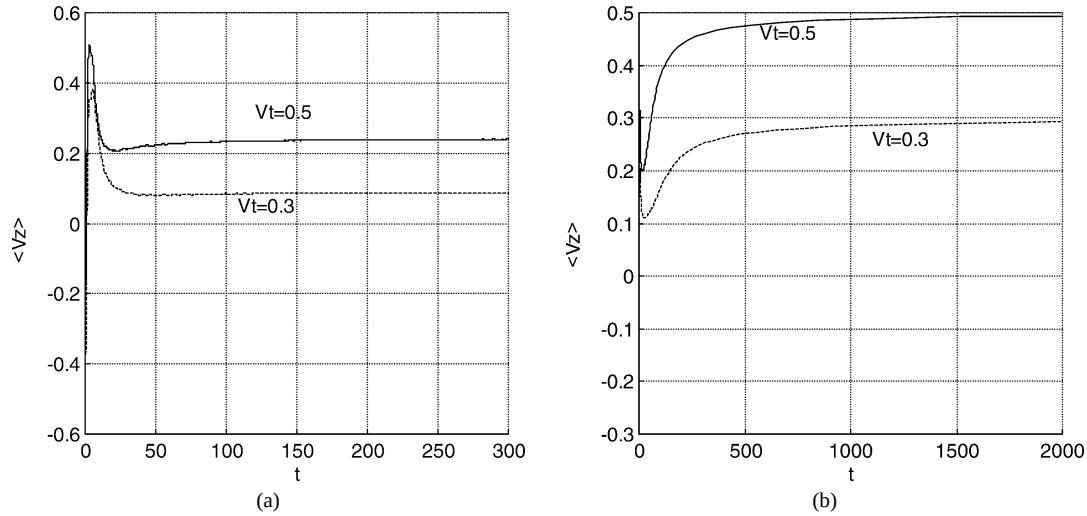

Fig. 5. Average fall velocity for non-inertial particles ($St = 0$). (a) $\theta = \pi/2$, $v_t = 0.3, 0.5$. (b) $\theta = \pi/4$, $v_t = 0.3, 0.5$.

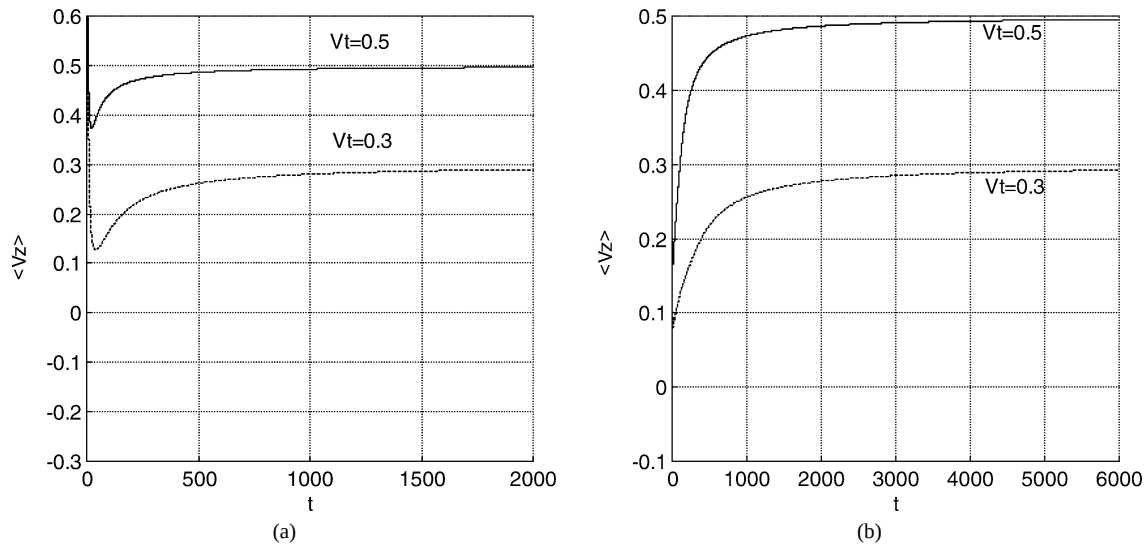

Fig. 6. Average fall velocity for inertial particles ($St = 0.5$). (a) $\theta = \pi/2$, $v_t = 0.3, 0.5$. (b) $\theta = \pi/4$, $v_t = 0.3, 0.5$.

the closed trajectories zone and the remaining fluid and the inertial particles released above the vortex will not reach the core of the vortex on account of the centrifugal forces acting on them.

Therefore if particles are released above the vortices some empty regions will appear and their geometry depends on the terminal velocity. As we have already seen, the radial distance of the equilibrium point $\boldsymbol{x}_{E2}$ increases in proportion to $R^2\Omega/v_t \sin\theta$; as a consequence the empty regions become wider as v_t decreases. Furthermore, as the Stokes number increases, the centrifugal force becomes greater and the empty region becomes wider.

Now, in Fig. 4, we show the particle trajectories for an inclined vortex ($\theta = \pi/4$). The plots of the trajectories related to the fixed axis $Oxyz$ are not very significant and the main features cannot be estimated, so we only include plots related to the $Ox2y2z2$ axis.

In these plots particles have been released in the same plane $z2 =$ constant. The most representative is the $Ox2y2$ plot, in which we can see the similitude with the horizontal vortex case: the projection of the trajectories on $Ox2y2$ plane are closed curves for non-inertial particles ($St = 0$); that is, the spatial trajectories of the particles is a type of helix. For inertial particles that projection on $Ox2y2$ plane is not a closed curve but the particle, in projection, moves outwards on curves that are spirals.

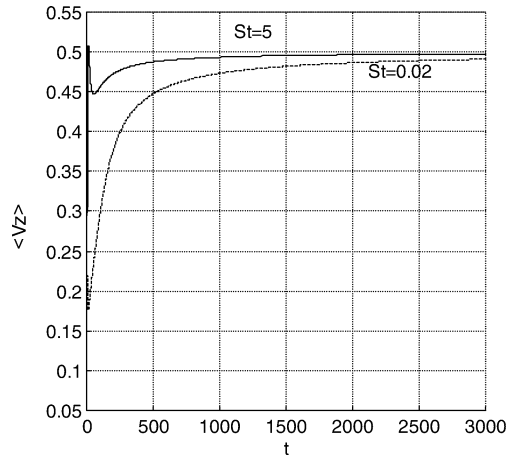

Fig. 7. Average fall velocity for $v_t = 0.5$, $St = 0.02$, 5.0, $\theta = \pi/4$.

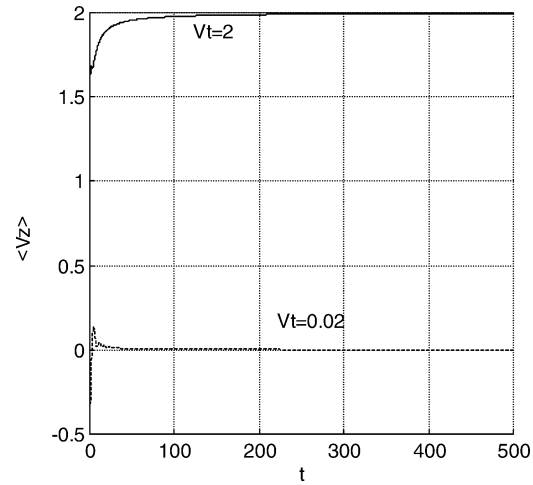

Fig. 8. Average fall velocity for $\theta = \pi/4$, $St = 0.5$, $v_t = 0.02$, 2.

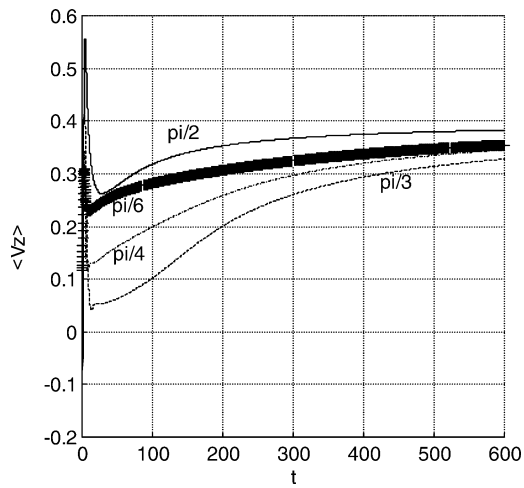

Fig. 9. Average fall velocity for $v_t = 0.4$, $St = 0.5$, $\theta = \pi/2$, $\theta = \pi/3$, $\theta = \pi/4$, $\theta = \pi/6$.

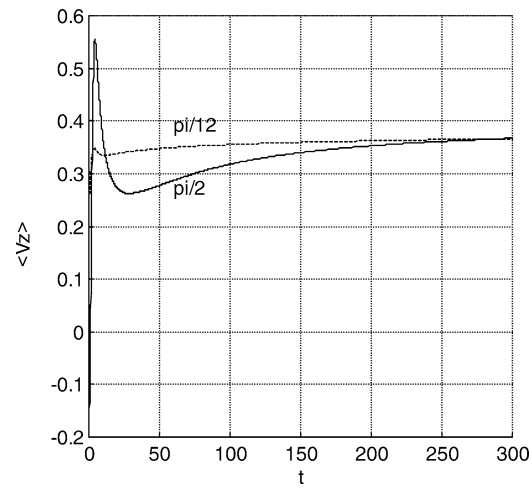

Fig. 10. Average fall velocity for $v_t = 0.4$, $St = 0.5$, $\theta = \pi/2$, $\theta = \pi/12$.

In an analogous way, there will be limit trajectories separating this zone of closed trajectories (in projection) and the remainder of the fluid field so particles released in some zones will not reach the central zone of the vortex and some empty regions will appear. In analogy with the horizontal case, the empty regions become wider as v_t decreases and as the Stokes number increases the centrifugal force becomes greater and the empty region becomes wider.

Comparing different nutation angles, as the nutation angle is smaller the closed and spirals trajectories zone is greater (in projection). The explanation is this: as that angle is smaller, particles have to cross a greater section of the vortex.

A fundamental difference between a horizontal vortex ($\theta = \pi/2$) and an inclined vortex ($\theta < \pi/2$) is the following: in the horizontal vortex case, particles always move in a plane perpendicular to the vortex axis and they never go out of that plane, but in the inclined vortex it does not happen that way.

We can see v_t has a component $v_t \cos\theta$ that "wants" to bring the particles out of the plane perpendicular to the vortex axis in which they are released and this effect is stronger as θ is smaller, because then $\cos\theta$ is greater. Therefore, as the vortex is more inclined the tendency of the particles to leave the plane perpendicular to the vortex axis in which they are is greater. It is obvious then, for $\theta = \pi/2$, a horizontal vortex, v_t has only one component (Oz direction) and particles always remain in the plane perpendicular to the vortex axis which they was.

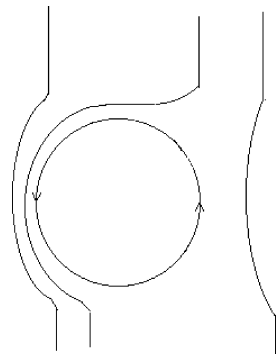

Fig. 11. Particle trajectories near a horizontal Rankine vortex.

4.2. Average fall velocity

For each case we have take a mesh of 500 equi-spaced particles in a plane perpendicular to the vortex axis and for the various combinations of the parameters θ, St, v_t, we have integrated the system (2.7) with the fluid velocity field (3.1) using a fourth order variable step size Runge–Kutta method [14] as we have already mentioned.

Fig. 5 shows the average fall velocity for non-inertial particles, various values of v_t and various nutation angles. When the vortex axis is inclined $\langle Vz\rangle$ has a tendency to asymptote to v_t but for a horizontal vortex (in the case of non-inertial particles) this does not happen (Fig. 5(a)). That is a consequence that particles have been taken in a plane perpendicular to the vortex axis and, as we have already seen, in this case v_t has no component that forces the particles to leave that plane, therefore the residence time of the particles in the vortex grows.

Fig. 6 shows the same plots for inertial particles ($St = 0.5$). In this case $\langle Vz\rangle$ has a tendency to asymptote to v_t even if the vortex is horizontal.

In Fig. 7 we can see the influence of the parameter St, that is, the influence of the particle inertia for an inclined vortex. We have taken two very different values of St to observe clearly the difference. The computational simulations confirm the expected results: when the inertia is large the asymptote v_t is reached faster for every nutation angle. Fig. 8 shows the influence of the dimensionless terminal velocity v_t for θ and St fixed. As v_t is smaller, the asymptote is reached faster. Finally, in Fig. 9 we show $\langle Vz\rangle$ versus t for St and v_t fixed and various values of the nutation angle θ.

The influence of θ is seen with sharpness in Fig. 10; for the same fixed values of St and v_t we plot $\langle Vz\rangle$ versus t for two very different values of the nutation angle. When θ is small (vortex very inclined) the asymptote v_t is reached faster because the velocity field (3.3) with $\Psi = 0$ is

$$\boldsymbol{u} = (\Omega/DEN)\big[(-y\cos\theta - z\sin\theta)\boldsymbol{i} + (x\cos\theta)\,\boldsymbol{j} + (x\sin\theta)\boldsymbol{k}\big] \tag{4.1}$$

with

$$DEN = 1 + \frac{x^2}{R^2} + \frac{(y\cos\theta + z\sin\theta)^2}{R^2} \tag{4.2}$$

and as $\sin\theta$ is small the Oz component of $\boldsymbol{u}$ is small. Furthermore, as $\sin\theta$ is small and $\cos\theta$ is big, the component of v_t that "wants" to keep the particles in the plane perpendicular to the vortex axis is small so the time over which the vortex takes action is small and the value v_t is reached soon.

In all the cases, there is an evident tendency of $\langle Vz\rangle$ to v_t. The explanation, which can be generalized for every angle, is easily seen for the horizontal vortex case, shown in Fig. 11. Particles falling on the left-hand side increase their average fall velocity because of the vortex action and particles falling on the right-hand side decrease their average fall velocity for the same reason, but considering an ensamble of particles over the whole field these effects are compensating so $\langle Vz\rangle \to v_t$.

5. General conclusions

Firstly, we have plotted the trajectories of particles near a Rankine vortex varying the Stokes number St, the dimensionless terminal velocity v_t and the nutation angle θ. We have obtained some qualitative results as in previous studies. Non-inertial particles ($St = 0$) can execute closed trajectories for every nutation angle but inertial particles ($St > 0$) do not execute closed trajectories and some empty regions appear; these empty regions become wider as v_t decreases; furthermore by increasing the Stokes number the centrifugal force becomes greater and the empty region becomes wider.

There is a fundamental difference between a horizontal vortex ($\theta = \pi/2$) and an inclined vortex ($\theta < \pi/2$); in the first case particles always move in a plane perpendicular to the vortex axis and they never go out of that plane but in the second case they do because of the influence of the $v_t \cos\theta$ component. This effect is stronger as θ is smaller.

Furthermore we have verified that decreasing the nutation angle results in a greater closed trajectories zone and in a greater spiral trajectories zone (in projection for $\theta < \pi/2$) because particles have to cross a wider section of the vortex.

Secondly, we have plotted the average fall velocity $\langle Vz \rangle$ versus time for various combinations of the parameters. $\langle Vz \rangle$ always has a tendency to asymptote to v_t except in the horizontal vortex case with non-inertial particles because particles have been taken in a plane perpendicular to the vortex axis and in this case v_t has no component to bring them out of that plane. We have verified that increasing the particle inertia leads to the asymptote v_t being reached faster, as we expect.

Our fundamental finding is the influence of the nutation angle with v_t and *St* fixed. As θ falls, v_t is reached faster because the Oz component of the Rankine vortex velocity is small and because the component of v_t that acts to keep the particle in a plane perpendicular to the vortex axis is small, so the time which the vortex takes action is small.

Acknowledgements

We are grateful to Dr. J. Dávila from Seville University for his instruction.

References

[1] P. Nielsen, On the motion of suspended sand particles, J. Geophys. Res. 89 (1984) 616–626.
[2] P.F. Tooby, G.L. Wick, J.D. Isaacs, The motion of a small sphere in a rotating velocity field: a possible mechanism for suspending particles in turbulence, J. Geophys. Res. 82 (15) (1977) 2096–2100.
[3] C.G. Du Toit, J.F.A. Sleath, Velocity measurements close to rippled beds in oscillatory flow, J. Fluid Mech. 112 (1981) 71–96.
[4] R. Perkins, J.F.A. Sleath, Near bed velocities in combined steady plus oscillatory flow, in: Proc. XXth Congress IAHR VII, 1983, pp. 173–177.
[5] T.R. Auton, The dynamics of bubbles, drops and particles in motion in liquids, Ph.D. Dissertation, University of Cambridge, 1983.
[6] K.J. Sene, J.C.R. Hunt, N.H. Thomas, The role of coherent structures in bubble transport by turbulent shear flows, J. Fluid Mech. 259 (1994) 219–240.
[7] R. Perkins, J.C.R. Hunt, Particle transport in turbulent shear flows, 1987, unpublished.
[8] J. Davila, J.C.R. Hunt, Settling of small particles near vortices and in turbulence, J. Fluid Mech. 440 (2001) 117–145.
[9] C.T. Crowe, J.N. Chung, T.R. Troutt, Particle interaction with vortices, in: Fluid Vortices, Kluwer Academic, 1995, Chapter 19.
[10] F. Clifford, Hardisty, Turbulence: Perspectives on Flow and Sediment Transport, Wiley, 1983.
[11] M.R. Maxey, J.J. Riley, Equation of motion for a small rigid sphere in a nonuniform flow, Phys. Fluids 26 (1983) 883–889.
[12] R. Clift, J.R. Grace, M.E. Weber, Bubbles, Drops and Particles, Academic Press, New York, 1978.
[13] E.J. Katz, Atmospheric difussion of settling particles with sluggish response, J. Atmos. Sci. 23 (1966) 159–166.
[14] W.H. Press, S.A. Teukolsky, W.T. Vettering, B.P. Flannery, Numerical Recipes in c. The Art of Scientific Computing, Cambridge University Press, 1992.